UDK 621.315.592

# Comparative morphology and photoluminescence of ZnO films obtained by SILAR and vacuum deposition methods

© S.V. Denisiuk[1], O.N. Kudanovich[1], N.I. Mukhurov[1], A.A. Khodin[1], E.A. Outkina[2], M.V. Meledina[2], A.A. Tabolich[3]

[1] State Scientific and Production Association „Optics, Optoelectronics and Laser Technology“, 220072 Minsk, Republic of Belarus
[2] Belarusian State University of Informatics and Radioelectronics, 220013 Minsk, Belarus
[3] Institute of Physics of the National Academy of Sciences of Belarus, 220072 Minsk, Republic of Belarus

E-mail: denicuk.sv@gmail.com

*Received May 3, 2024*
*Revised July 26, 2024*
*Accepted October 30, 2024*

Functional zinc oxide layers were obtained on substrates of anodic aluminium oxide with methods SILAR (Successive Ionic Layer Adsorption and Reaction) and thermal oxidation in oxygen-containing medium zinc films deposited in vacuum. Morphology of surface and cleaved facets were studied. Photoluminescence spectra of samples were obtained. Differences in surface structure and optical properties were determined between polycrystalline ZnO films obtained in different conditions.

**Keywords:** zinc oxide, nanofilaments, photoluminescence, aluminium oxide.

DOI: 10.61011/SC.2024.11.59951.6549A

## 1. Introduction

Zinc oxide is a direct band gap semiconductor with a band gap width of 3.27 eV, which has *n*-type conductivity due to interstitial zinc and oxygen vacancies, and a significant exciton energy ($\sim 60$ meV). Under normal conditions, ZnO mostly has a wurtzite crystal structure. Zinc oxide has two luminescence peaks: at $\sim 378$ nm, which corresponds to the edge of the absorption band and exciton recombination, and at $\sim 562$ nm, which is associated with the presence of oxygen vacancies [1]. A distinctive feature of ZnO is the ability to form nanoparticles of various shapes: nanowires, nanorods, nanoplates, etc. [2]. The specific features of electrophysical and optical properties of zinc oxide allow the use of ZnO films in photodetectors, solar cells, thin-film transistors, as well as in the production of flat panel displays, piezoelectric devices and gas sensors [3,4]. Both physical methods, such as pulsed laser or magnetron sputtering, and chemical methods, such as sol-gel technology, spray pyrolysis, hydrothermal and CVD methods [5,6], are used to produce ZnO.

## 2. Experimental

ZnO film samples were formed on nanoporous anodic aluminium oxide (AOA) substrates obtained by anodizing aluminium in 3% oxalic acid solution to a thickness of $40-42\,\mu$m. After anodization, the metal base was removed and then the substrates were annealed to stabilise their parameters. One side of the substrate is a porous surface with pores $60-75$ nm in diameter, and the reverse side is porous (barrier layer) [7].

Cationic and anionic precursors were used to form zinc oxide film by SILAR (Successive Ionic Layer Adsorption and Reaction) method. A 0.1 M aqueous solution of $ZnSO_4$ with addition of $NH_4OH$ was used as the cationic precursor. A 1% solution of $H_2O_2$ was used as the anionic precursor. 10 cycles of dipping were performed to form a homogeneous ZnO film. A part of the samples was subjected to heat treatment at 300°C for 1 h. The second technique for obtaining ZnO films includes the stages of vacuum deposition of the metal film and its thermal oxidation. Zinc films were deposited on the substrates using a vacuum magnetron sputtering unit „Oratoria 9“ to a thickness of $1.2-1.4\,\mu$m, after which they were subjected to thermal oxidation in a SNOL 6.7/1300 muffle electric furnace at temperatures ranging from 300 to 600°C.

The morphology of the samples was studied using a Hitachi S-4800 scanning electron microscope (SEM). Photoluminescence (PL) spectra were recorded at room temperature in the range of $310-950$ nm using a HORIBA iHR320 spectrometer (Japan) with excitation by Xe lamp radiation in the range of $\sim 350-520$ nm.

## 3. Results and discussion

The SILAR-derived zinc oxide layers on AOA substrates are fine-grained polycrystalline films with a thickness of $1-1.5\,\mu$m. SEM images of zinc oxide deposited on the porous side of the alumina substrate show a film consisting

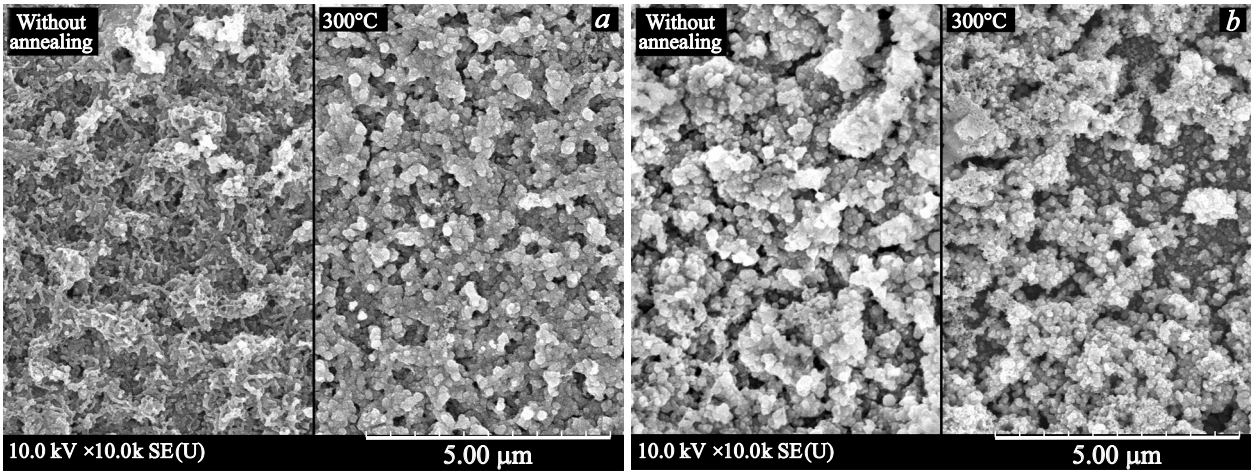


**Figure 1.** SEM images of different sections of ZnO films obtained by SILAR method on anodic aluminium oxide substrate: *a* — ZnO on the porous side of the substrate before and after annealing; *b* — ZnO on the barrier layer of the substrate before and after annealing.

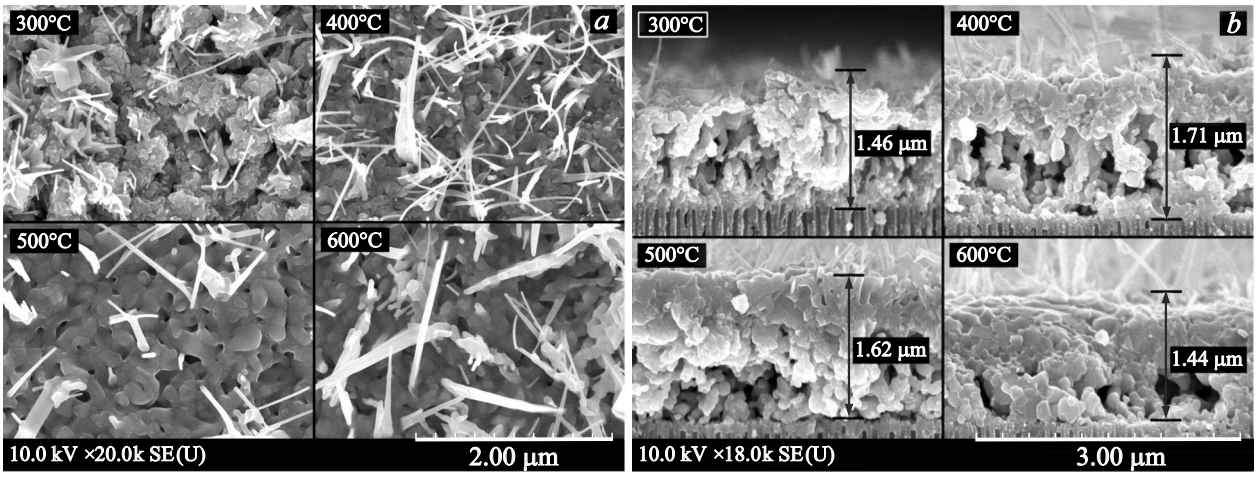


**Figure 2.** SEM images of surface and cleaved facet samples of ZnO films on nanoporous $Al_2O_3$: *a* is a surface morphology of ZnO films obtained by oxidation at temperatures of 300, 400, 500 and 600°C; *b* are sample cleaved facets with ZnO films obtained by oxidation at temperatures of 300, 400, 500 and 600°C.

of conglomerates and individual spherical particles with diameters ranging from 100 to 400 nm, as well as areas with disordered porous structure, an interstitial distance of 50–75 nm and grain sizes ranging from 100 to 300 nm (Figure 1, *a*). After annealing at 300°C temperature, the surface image of the samples shows the porous structure of ZnO films and the enlargement of the film grains up to 250–500 nm. At the same time, areas of peeling of the oxide film from the substrate are observed. The zinc oxide film deposited on the barrier side of the substrate has a fine-grained disordered structure with the size of individual grains from 50 to 300 nm and inclusions of fragments of thin films. After thermal treatment at 300°C the SEM image of the ZnO film surface shows no noticeable changes in the film structure or in the sizes of its constituent grains (Figure 1, *b*).

During air oxidation of the Zn layer formed on the porous surface of the AOA substrate at the temperature 300°C a polycrystalline film (Figure 2, *a*) is formed, which has a porous microrelief consisting of conglomerates of irregularly shaped particles with characteristic dimensions of 200–400 nm. One- and two-dimensional nanoparticles in the form of nanofilaments and nanoplates are formed on the film surface. The SEM image of the sample cleaved facet shows that the formation of nanoparticles occurs only on the film surface (Figure 2, *b*). The nanofilament diameter and nanoplate thickness are $\sim 20-30$ nm, while the length of nanofilaments can reach 1 $\mu$m. An increase in the oxidation temperature to 400°C causes the formation of an oxide film with a more homogeneous surface and the increase of the nanofilament number and length up to 2.0 $\mu$m (Figure 2, *a*). The number of nanoplates per surface unit decreases and

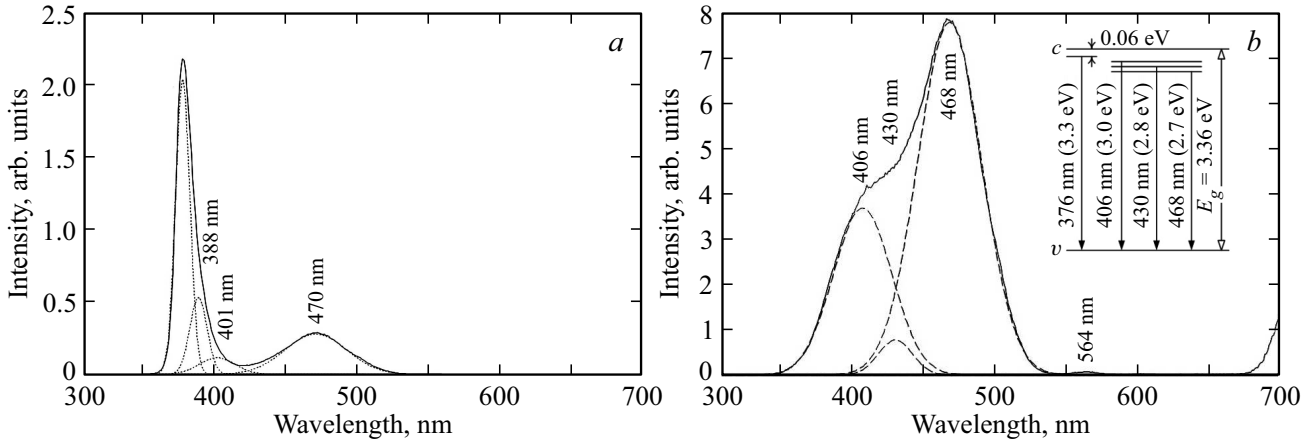


**Figure 3.** Photoluminescence spectra of $ZnO/Al_2O_3$ film structures after oxidation of Zn films at 400°C ($a$) and 500°C ($b$). The inset shows the main PL transitions in ZnO involving exciton states and interstitial Zn atoms.

the remaining ones show signs of being transformed into nanofilament conglomerates. The SEM image of the sample cleaved facet reveals three layers of the film: a porous base $\sim 1\,\mu$m thick, a dense quasiplanar surface $0.5-0.7\,\mu$m thick, and ZnO nanofilaments up to $1.5\,\mu$m long growing on it (Figure 2, $b$).

SEM images of the surface of samples obtained by oxidation of Zn film on the surface of $Al_2O_3$ at the temperature of 500°C, show a porous film microrelief consisting of partially fused grains of rounded shape with the size of individual particles 200–300 nm (Figure 2, $a$). Nanofilaments with diameters ranging from 30 to 200 nm are formed on the surface of the ZnO film. Compared to the samples obtained at 300 and 400°C, a change in the nanofilament diameter from the apex to the base is observed. At the oxidation temperature 600°C a polycrystalline film with similar morphology is formed, the main difference being an increase in the density of nanofilaments per unit surface area (Figure 2, $a$). The nanofilament diameters range from 50 to 200 nm with lengths from 200 nm to $2\,\mu$m with an increase in the average diameter. The three-layer film structure typical of the samples obtained at 400°C, temperature is retained at annealing temperatures of 500 and 600°C (Figure 2, $b$).

The ZnO nanofilaments were also formed in the samples obtained by thermal oxidation, in contrast to the samples obtained by SILAR technique. The photoluminescence characteristics of the latter were not considered in this paper. The PL spectra of ZnO film samples with nanofilaments on a nanoporous AOA substrate (Figure 3) reveal the presence of bands that are typical of hydroxide/porous $Al_2O_3$ ($\sim 450/690$ nm), obtained by anodising in oxalic acid, which is consistent with the results presented in [8–10]. This photoluminescence may have originated from the transformation of anionic impurities (oxalates) embedded in aluminium oxide into active emission centres, as well as structural defects in $Al_2O_3$, in particular $F/F^+$-centres [8,11,12]. For ZnO samples oxidized at 400°C the PL band at $\sim 400$ nm is weakly expressed (Figure 3, $a$), whereas for samples oxidized at 500°C this band is predominant (Figure 3, $b$). Photoluminescence of ZnO involving exciton transitions ($\sim 376$ nm) was observed at the oxidation temperature of 400°C (Figure 3, $a$) and was not observed at the oxidation temperature of 500°C (Figure 3, $b$). At the same time, in the second case, a series of 406/430/468 nm bands typical of transitions involving interstitial defects $I_{Zn}/I_{Zn}^+$ [13]. Thus, thermal oxidation of Zn films on nanoporous anodic aluminium substrates yields different PL results, where after oxidation at 500°C the PL transitions involving excess interstitial Zn prevail.

## 4. Conclusion

Both of the above methods allow obtaining functional zinc oxide layers, which can be used in various microelectronics devices. At the same time, the combination of methods of metal deposition in vacuum followed by thermal oxidation allows to obtain ZnO films of different topology with surface nanofilaments, the size and shape of which depend on the production conditions. The results of studying the photoluminescence of ZnO films with nanofilaments indicate a transition from the exciton mechanism of luminescence to predominantly interstitial Zn ion luminescence with the increase of oxidation temperature from 400 to 500°C with a change in the micromorphology of nanofilaments formed on the quasiplanar layer of zinc oxide.

### Funding

The study was funded by the Belarusian Republican Foundation for Fundamental Research, grant T23ME-045.

### Conflict of interest

The authors declare that they have no conflict of interest.

## References

[1] D. Hong, G. Cao, X. Zhang, J. Qu, Y. Deng, H. Liang, J. Tang. Electrochimica Acta, **283**, 959 (2018). DOI: 10.1016/j.electacta.2018.05.051
[2] E.K. Droepenu, B.S. Wee, S.F. Chin, K.Y. Kok, M.F. Maligan. Biointerface Res. Appl. Chem., **12** (3), 4261 (2022). DOI: 10.33263/briac123.42614292
[3] M.A. Borysiewicz. Crystals, **9** (10), 505 (2019). DOI: 10.3390/cryst9100505
[4] A.V. Marikutsa, N.A. Vorob'eva, M.N. Rumyantseva, A.M. Gas'kov. Russian Chem. Bull., **66** (10), 1728 (2017). DOI: 10.1007/s11172-017-1949-7
[5] V.R.V. Gopal, S. Kamila. Appl. Nanoscience, **7** (3–4), 75 (2017). DOI: 10.1007/s13204-017-0553-3
[6] I.A. Nagornov, A.S. Mokrushin, E.P. Simonenko, N.P. Simonenko, Ph.Yu. Gorobtsov, V.G. Sevastyanov, N.T. Kuznetsov. Ceramics International, **46** (6), 7756 (2020). DOI: 10.1016/j.ceramint.2019.11.279
[7] Y. Patel, G. Janusas, A. Palevicius. Materials Today: Proceedings, **57** (2), 630 (2022). DOI: 10.1016/j.matpr.2022.02.044
[8] G.S. Huang, X.L. Wu, Y.F. Mei, X.F. Shao. J. Appl. Phys., **93** (1), 582 (2003). DOI: 10.1063/1.1529075
[9] G. Rani. J. Korean Ceram. Soc., **58**, 747 (2021). DOI: 10.1007/s43207-021-00151-3
[10] S.C. Khoobaram, C.-H. Choi, S. Chidangil, S.D. George, S.D. George. Nanomaterials, **12** (3), 444 (2022). DOI: 10.3390/nano12030444
[11] L. Cantelli, J.S. Santos, T.F. Silva, M.H. Tabacniks, A.O. Delgado-Silva, F. Trivinho-Strixino. J. Luminesc., **207**, 63 (2019). DOI: 10.1016/j.jlumin.2018.10.015
[12] N. Mukhurov, S. Zhvavyi, Sergei N. Terekhov, A. Panarin, I.F. Kotova, P. Pershukevich, I. Khodasevich, I. Gasenkova, V. Orlovich. J. Appl. Spectrosc., **75** (2), 214 (2008). DOI: 10.1007/S10812-008-9026-5
[13] K. Bandopadhyay, J. Mitra. RSC Adv., **5**, 23540 (2015). DOI: 10.1039/C5RA00355E

*Translated by J.Savelyeva*